Arab J. Nucl. Sci. Appl., Vol. 56, 3, 166-174 (2023)

ISSN 1110-0451

Arab Journal of Nuclear Sciences and Applications

Web site: ajnsa.journals.ekb.eg

(E S N S A)

Preparation and Stabilization of Monoclinic Zirconia by Yttria through Mechanical Alloying

W. Eldesouky[1*], A. AbdelKarim[1], H. M. Abd El Aziz[2], E. S. Mosa[2]

(1) Nuclear Materials Authority, Cairo, Egypt

(2) Mining and Petroleum Engineering Department, Faculty of Engineering Al Azhar University, Cairo, Egypt.

ARTICLE INFO

Article history:

Received: 7th Sept. 2022

Accepted: 31st Dec. 2022

Keywords:

Zirconia;
Alkali fusion;
Yttria;
Yttria stabilized zirconia;
Mechanical alloying;
Phase transformation.

ABSTRACT

Yttria-stabilized zirconia is a vital material for a variety of high-tech industrial applications. Fully stabilized zirconia is an excellent material for manufacturing of solid electrolyte for solid oxide fuel cell. In the present study, high purity zirconia was successfully synthesized from Egyptian zircon. The produced zirconia was subsequently fully stabilized by 10 mol% yttria via mechanical alloying. Mechanical alloying was conducted in a planetary ball mill with; stainless steel milling assembly, at a rotation speed of 350 rpm, and ball to powder weight ratio of 10. The effect of milling time (up to 32 h) on phase transformation was studied. Characterization of the as prepared zirconia and milled samples was conducted by X-ray diffraction, scanning electron microscopy, and energy dispersive X-ray analysis. The obtained results revealed that, the crystal structure of the prepared zirconia is monoclinic. The degree of stabilization and the level of contamination increase gradually with the course of milling. Under the described conditions, the required time for full stabilization was 32 h. The produced powder is nanocrystalline (13.7 nm) with a submicron particle size.

INTRODUCTION

Egypt is endowed with large resources of black sand placer deposits which contain important heavy minerals e.g. zircon ($ZrSiO_4$) [1]. Zircon is the major source of zirconium metal and compounds such as zirconium oxide (ZrO_2) which usually is called zirconia. It is one of the most important ceramic oxides thanks to the exceptional combination of its properties; high melting point (2710°C), low thermal conductivity, high wear and corrosion resistance, and chemical inertness. These unique properties allow it to be used in a wide range of important industrial applications [2]. Pure ZrO_2 is typically polymorphic, and upon heating it transforms from monoclinic (m-ZrO_2) to tetragonal (t- ZrO_2) at 1170°C then to cubic (c- ZrO_2) at 2370°C. During cooling, it comes back from c- ZrO_2 to t- ZrO_2 which is accompanied by a little change in volume. Nevertheless, from t- ZrO_2 to m- ZrO_2 a significant volume increase (≈ 5%) takes place, which leads to cracking and failure of the sintered part. As a result, pure ZrO_2 can only be used in the powder form, and industrial ZrO_2 components are impossible to fabricate [3, 4]. Fortunately, t or c- ZrO_2 can be stabilized at room temperature by doping m-ZrO_2 with oxides which have cubic crystal structure and their ions have an ionic radius close to that of Zr^{4+} [5]. Yttria (Y_2O_3), calcia (CaO), magnesia (MgO), and Ceria (CeO_2) are the most frequently used stabilizers [6]. Once stabilized, the crystal structure of Stabilized Zirconia (SZ) will still the same from room temperature to melting point. This allows SZ powder to be compacted and sintered to produce important industrial items [7]. The primary function of stabilization was only to prevent phase transformation. In addition, SZ offered excellent mechanical and electrical properties depending on the type and amount of the stabilizer [8]. Yttria-Stabilized Zirconia (YSZ) is one of the most studied high-performance ceramics due to its high hardness, low thermal conductivity, high toughness, excellent ionic conductivity as well as high wear, corrosion, and radiation resistance. Therefore, YSZ finds a very wide range of applications like thermal barrier coatings, solid electrolyte for solid oxide fuel cells, oxygen sensors, nuclear waste storage, Prosthetic implants, etc. [9, 10].

Mechanical Alloying (MA) is a solid-state powder processing technique in which powder particles are

Corresponding author: eng.wageeh_eldesouky@yahoo.com

DOI: 10.21608/ajnsa.2022.161293.1634

subjected to repeated cold welding, fracturing, and rewelding in a high-energy ball mill [11]. MA has historically been, and is also currently, one of the most effective techniques for the preparation of a very wide range of important materials e.g. ceramics [12, 13]. MA is considered a mechanochemical process because the mechanical energy is used to initiate structural changes, chemical reactions, and also a refinement of grain size [14]. MA is a simple, effective, cheap, and easy handling technique. It is also applicable to a wide range of different types of materials and it is able to produce large quantities [15, 16]. YSZ can be effectively produced by MA of ZrO_2 with the required amount of Y_2O_3 based on the desired phase.

Phase transformation of m- ZrO_2 to t- ZrO_2 or c- ZrO_2 during MA without the addition of any stabilizer was studied by Gajovic et al. [17]. It was found that, under given milling conditions, ball milling had a negligible influence on the transition from m to t-ZrO_2. Also, when WC milling assembly is used with BPR (20: 1) and rotation speed (200 rpm), only partial transformation occurred after 110 h [18]. However, under more severe conditions (rotation speed (750rpm), ball to powder ratio (25: 1), and milling time (80h), Zakeri et al. [13] achieved 80% phase transformation to t-ZrO_2. The word" without any stabilizer" means that, the milling assembly is made from zirconia to prevent the contamination. Hardened steel, hardened chromium steel, and Stainless Steel (SS) are common milling assemblies. Due to the nature of ZrO_2 and intense milling conditions, iron, nickel, and chromium cations are introduced to the powder due to wearing. Contaminants, especially iron can act as a stabilizer as observed by Stefanic et al. [19] so, the phase transformations occurred in some studies [20– 23] are clearly attributed to the stabilization effect of iron.

Preparation of SZ via MA without stabilizers requires severe conditions and long times. Addition of stabilizers like CaO, MgO, or Y_2O_3 to m-ZrO_2 can result in a significant decrease in the milling time and intensity regardless of the type of milling assembly. Different studies [24– 29] approved that, YSZ can be prepared via MA of m- ZrO_2 with a suitable amount of stabilizer. Thanks to its high ionic conductivity and chemical and mechanical stability at high temperatures, cubic YSZ is the most widely used material for the preparation of the solid electrolyte for solid oxide fuel cell [30].

However, in most of the previous studies, standard powders were used, which aims to obtain a high purity ZrO_2 from zircon mineral. Furthermore, cubic YSZ will be prepared via MA of the produced ZrO_2 and 10 mol% of Y_2O_3. Preparation of such important material can increase the economic value of Egyptian raw materials.

MATERIALS AND METHODS

2.1 Materials

The starting material to produce zirconia is zircon sand, its chemical composition is shown in Table (1). High purity yttria (99.99%) (Alpha Chemika, India) was used as a stabilizer. All used chemicals were of analytical grade and were used without further purification.

2.2 Fabrication of Commercial Zirconia

The fabrication of commercial zirconia from zircon was carried out in three main steps, as follows: (i) A sample of Rosetta zircon concentrate was mixed with sodium hydroxide in a ratio of 1: 1.4 and charged to a 316-L SS crucible (height = 25 cm, diameter = 15 cm). The crucible was then Put into the electric furnace where the fusion reaction took place. Fusion temperature was adjusted at 650℃ and continued for 2.5 h. The fusion product was washed (i.e., water/solid ratio 4:1) and stirred for 2 h to dissolve the water-soluble sodium silicate formed (Na_2SiO_3). The mixture was filtered out, and the residue (Na_2ZrO_3; frit) was washed several times with DIW and dried at 100℃ for 12 h. (ii) Then, the dried sodium zirconate was leached with HCl (6 M) at 90℃ and 1: 2 solid liquid ratio to produce zirconium oxychloride octahydrate ($ZrOCl_2.8H_2O$), which was turned into the crystalline form by cooling the solution. The formed crystals were separated from the mother liquor by decantation followed by filtration and finally drying in air to obtain white powder crystals of $ZrOCl_2.8H_2O$. (iii) Finally, the obtained crystals were dissolved in DIW and zirconium hydroxide ($Zr(OH)_4$) was precipitated at pH- 9 by the addition of ammonia solution (NH_4OH). The produced $Zr(OH)_4$ was washed, dried at 105℃ for 12 h, and calcined at 900℃ for 2 h to produce ZrO_2.

Table (1): Chemical composition of zircon sand

Constituent	ZrO_2	HfO_2	SiO_2	Fe_2O_3	TiO_2	P_2O_5	Al_2O_3	REO	U_3O_8	ThO	MgO	CaO
Wt. %	65.50	1.56	32.23	0.14	0.22	0.13	0.06	0.07	0.04	0.02	0.02	0.01

2.3 Synthesis of YSZ via MA

The produced ZrO_2 in the above step was used as precursor for the synthesis of YSZ. It was mixed with 10 mol% Y_2O_3 (99.99%) to produce cubic YSZ. The MA process was carried out in a Fritsch planetary ball mill "Pulverisette 7" which is equipped with SS pots and balls. Milling conditions were; rotation speed (350 rpm), milling atmosphere (air), ball/powder weight ratio (10: 1), and milling time (32 h).

Characterization of the prepared ZrO_2 and milled samples (8, 16, 24, and 32 h) was conducted by means of X-Ray Diffraction (XRD) (Malvern Panalytical Empyrean-2020 Netherlands). A monochromatic Cu-K radiation with λ= 0.154 nm was used. The scanning position was at 2θ with a step of 0.02 (2θ)/Sec. Scanning Electron Microscopy (SEM), and Energy Dispersive X-ray spectrometry (EDX) were performed using a scanning electron microscope model (FE-SEM; SEM-JEOL JSM5800-LV), that equipped with a unit of EDX. For crystallite size and microstrain calculation, the Williamson–Hall (WH) method was used. In this method, crystallite size (*Dv*) and the microstrain (ε) are obtained from WH plot which is drawn between ($B\cos\theta$ versus $4\sin\theta$). The slope of the line is the value of microstrain, while the crystallite size is calculated from equation (1).

$$Dv\ (\text{nm}) = \frac{k\lambda}{\text{y intercept}} \qquad \textbf{(1)}$$

Where, k is the shape factor and usually considered 0.9 and λ is the wave length of x-ray (0.15406 nm) [25].

RESULTS AND DISCUSSION

3.1 Fabrication of commercial zirconia

Alkali fusion is the most widely used method to breakdown zircon sand. The reaction product of alkali fusion is friable and caustic powder (frit). Frit consists of sodium zirconate (Na_2ZrO_3), sodium silicate (Na_2SiO_3, Na_4SiO_4), sodium zirconium silicate (Na_2ZrSiO_5), and unreacted zircon as obtained by XRD pattern which is shown in Figure (1). These products of alkali fusion were obtained according to equations (2-4).

$$ZrSiO_4 + 2NaOH \rightarrow Na_2ZrSiO_5\ (\text{Insoluble}) + H_2O \qquad \textbf{(2)}$$

$$ZrSiO4 + 4NaOH \rightarrow Na2ZrO3\ (Insoluble) + Na2SiO3\ (Soluble) + 2H2O \qquad \textbf{(3)}$$

$$ZrSiO4 + 6NaOH \rightarrow Na2ZrO3 + Na4SiO4\ (Soluble) + 3H2O \qquad \textbf{(4)}$$

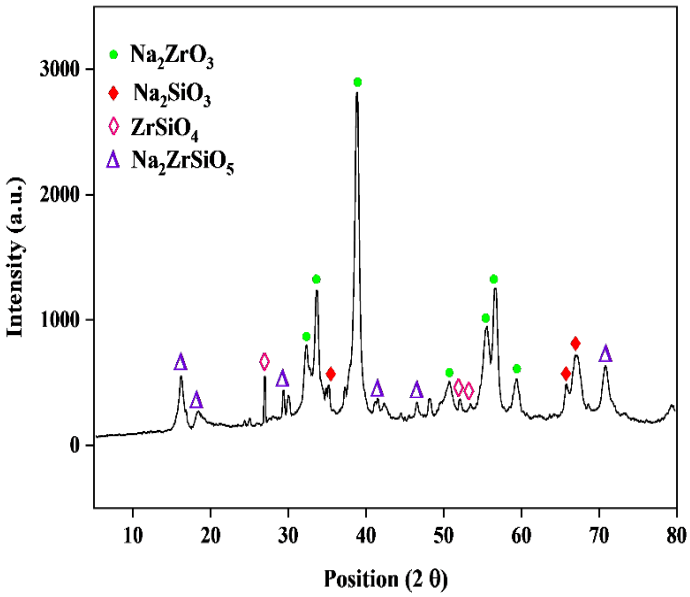

Fig. (1): XRD pattern of the product of alkali fusion

After washing, drying, and filtration, all soluble compounds were removed and the insoluble Na_2ZrO_3 was hydrolyzed to $ZrO(OH)_2$ according to equation (5). While Na_2ZrSiO_5 is water insoluble and does not hydrolyze in water.

Subsequently, zirconyl chloride ($ZrOCl_2.8H_2O$) was obtained by leaching the dried residue with HCl in accordance with equations (6) and (7). Here, the efficiency of decomposition was calculated by dividing the weight of unreacted zircon by the weight of the starting zircon, and it reached 94%. The XRD pattern of $ZrOCl_2$ is clearly shown in Figure (2).

$$Na_2ZrO_3 + 2H_2O \rightarrow ZrO(OH)_2 + 2NaOH \qquad \textbf{(5)}$$

$$ZrO(OH)_2 + 2HCl \rightarrow ZrOCl_2 + 2H_2O \qquad \textbf{(6)}$$

$$Na_2ZrSiO_5 + 4HCl \rightarrow ZrOCl_2 + 2NaCl + H_2SiO_3 + H_2O \qquad \textbf{(7)}$$

The obtained $ZrOCl_2$ crystals were water leached then treated with ammonium hydroxide to precipitate zirconium hydroxide according to equation (8). Finally, zirconium hydroxide was washed, dried for 12 h and calcined at 900°C for 2 h producing zirconia according to equation (9).

$$ZrOCl_2.8H_2O + 2NH_4OH \rightarrow ZrO(OH)_2.6H_2O + 2NH_4Cl \qquad \textbf{(8)}$$

$$ZrO(OH)_2 \xrightarrow{\text{Calcination}} ZrO_2 \qquad \textbf{(9)}$$

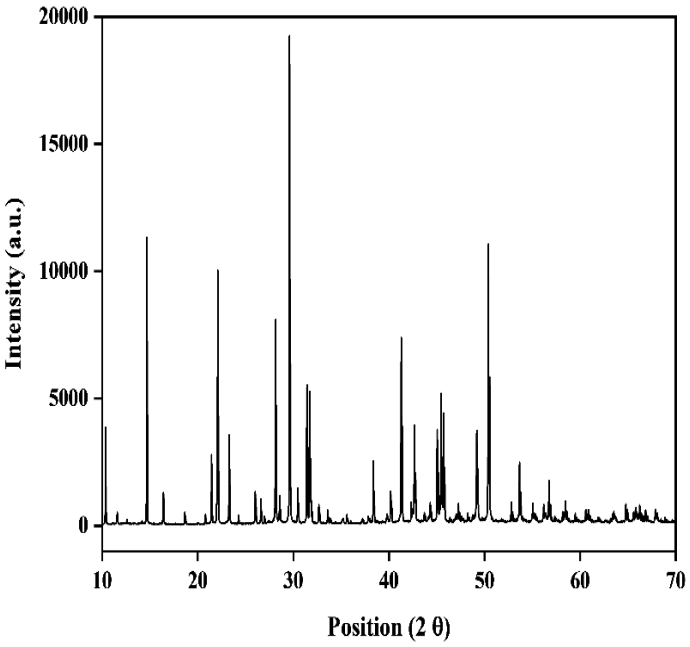

Fig. (2): XRD pattern of zirconium oxychloride

The XRF analysis of the prepared ZrO_2 is represented in Table (2), which indicates that, a product with significant purity was obtained. Hence, hafnium is very similar to zirconium in chemical and metallurgical properties [7], and it will not be considered as an impurity. So, it can be concluded that the obtained purity is more than 99%.

The crystal structure of fabricated ZrO_2 is investigated by X-ray diffraction (XRD). The XRD pattern of the as prepared ZrO_2 as compared with JCPDS PDF No. 37-1484, space group P21/c, a = 0.5145, b = 0.5212, c = 0.5312 nm, β = 99.218 is shown in figure 3. The diffractogram shows the domination of m-ZrO_2 as the major phase (95%) which shows several prominent reflections at 2θ values of about 24.45˚, 29.19˚, 31.46˚, 34.244˚, 35.29˚, 44.67˚, and 50.13˚. These findings are well consistent the referencing diffraction data. Also, a small reflection of c or t-ZrO_2 which counts about (5%) is detected at 2θ of 30.28˚ and denoted as (♦). The presence of suck peak may be attributed to the effect of impurities (Fe, Ca, and Mg) and high temperature calcination (900℃).

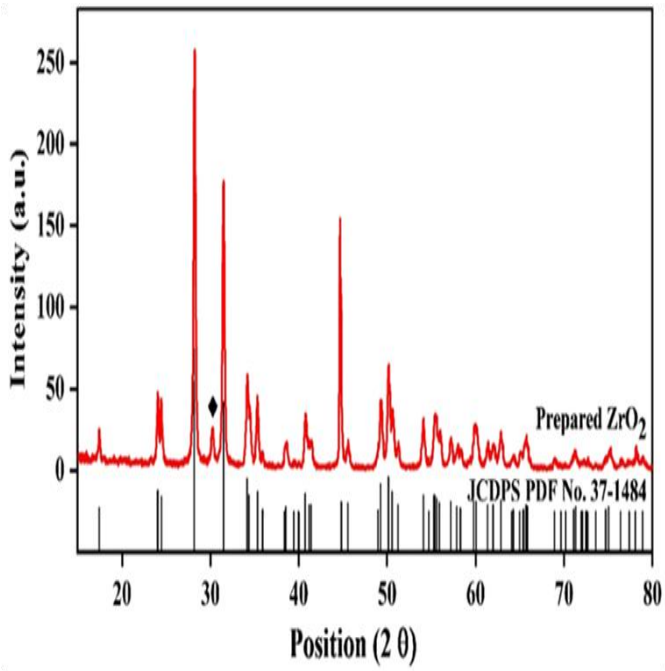

Fig. (3): X-ray diffraction pattern of prepared zirconia against the reference pattern

A SEM micrograph of as prepared ZrO_2 is represented in Figure (4). It reveals that the powder is made up of fine and agglomerated particles. The effect of high calcination temperature (900°C) is the reason for such agglomeration.

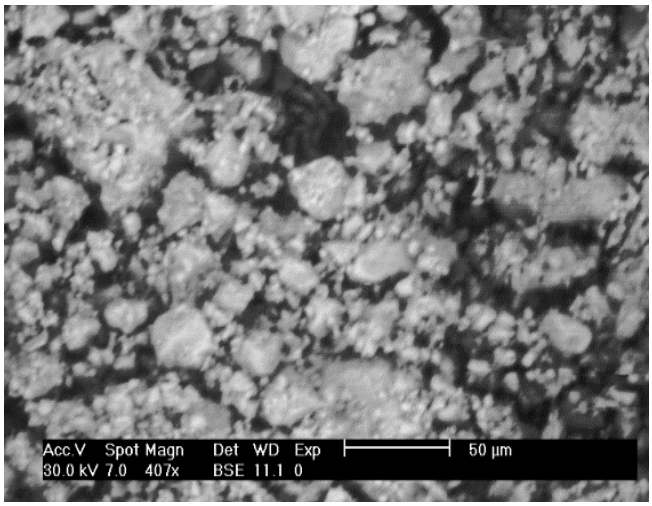

Fig. (4): A SEM micrograph of prepared zirconia

Table (2): Chemical composition of prepared ZrO_2

Component	$ZrO_2 + HfO_2$	SiO_2	Fe	Ti	Ca	U	Th	Mg	Na	K
Concentration	**wt.%**		**ppm**							
	99.62	0.35	48	510	85	< 10	< 10	95	66	75

3.2 Preparation of YSZ via MA

Ball milling was conducted in a planetary ball mill with SS milling assembly. This mill consists of one turn disc with two milling bowls. The disk rotates in one direction while the bowls rotate reversely, which creates centrifugal forces acting in opposite directions. As a result, the milling media and charged powders alternately roll on the vial's inner wall and are lifted and thrown across the bowl at high speeds as schematically presented in Figure (5).

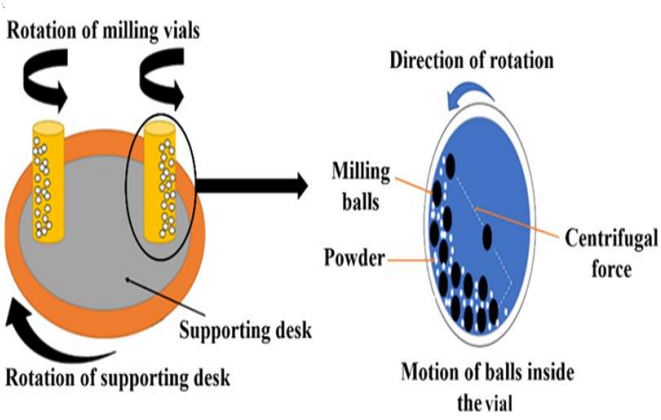

Fig. (5): schematic diagram of the mechanism of milling in planetary ball mill

The XRD patterns of milled powders for, 8, 16, 24, and 32 h are shown in Figure (6). When comparing the pattern of as- prepared ZrO_2 with that of 8 h, a significant peak broadening occurred and the strong peaks of m-ZrO_2 are significantly decreased. This is due to the grain size reduction and increased microstrains because of milling. Reduction in crystallite size increases the chemical reactivity and surface energy of the powder. Also, crystalline defects and structural disorder favor the diffusion of Y^{3+} ions into m- ZrO_2 lattice and atomic rearrangements. All these factors led to stabilization of high temperature cubic phase. This is indicated by the new formed peaks at about *2θ* values of 30˚, 34.7˚, 50˚, and 59.9˚ as well as the absence of c-Y_2O_3 peaks. All these findings mean that, MA is going well. The stabilization is accomplished by replacing the Zr^{4+} ions from the ZrO_2 matrix with bigger Y^{3+} ions. Since Y has one less valence electron than Zr, oxygen vacancies are created in the matrix to maintain neutral electronegativity. The presence of O vacancies enables YSZ to conduct O^{2-} ions. Tetragonal and cubic zirconia structures are very similar, which makes the identification of each phase very difficult [31]. So, the new peaks will be denoted as SZ. As indicated from the sample milled for 8 h, MA resulted in a significant peak broadening, which makes subsequent interpretation and calculations more difficult. So, for longer milling times; 16, 24, and 32 h, the samples were annealed for 3 h at 800°C to enhance the crystallinity and make interpretation and calculations easier. This is relevant from the sharpness and intensities of peaks.

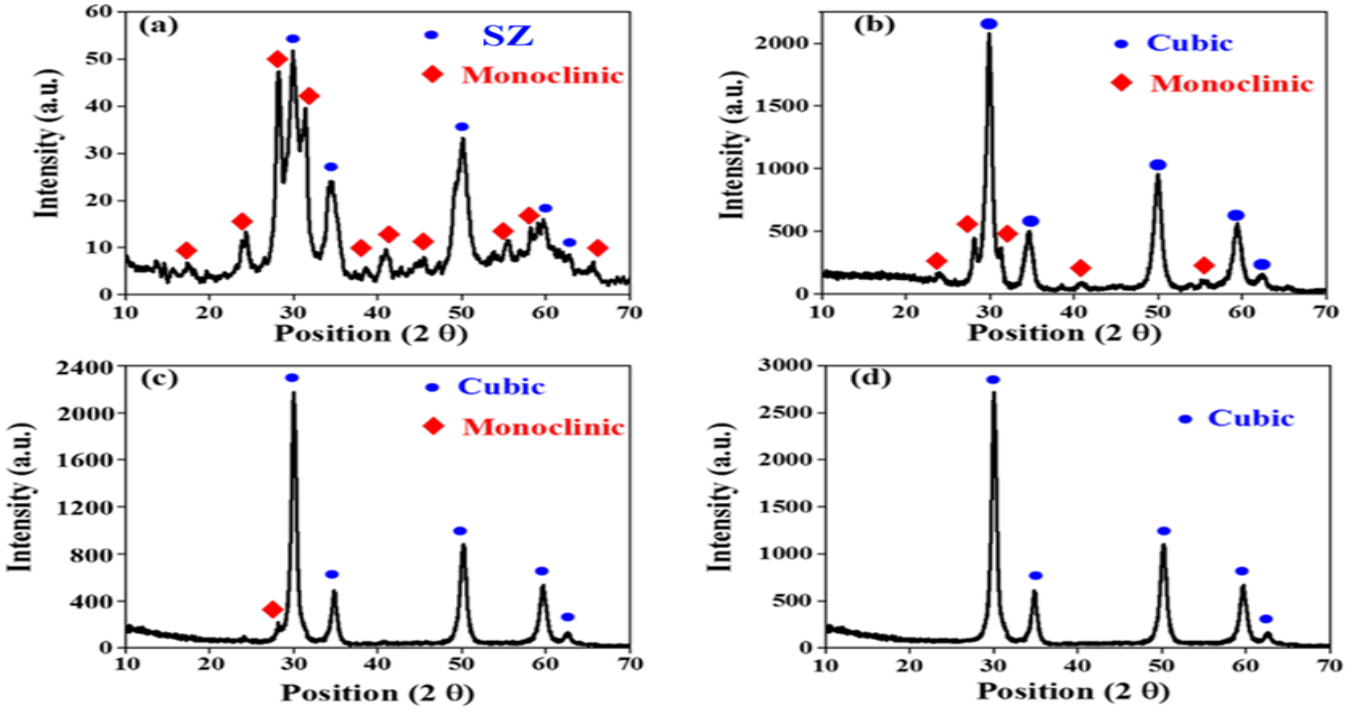

Fig. (6): XRD patterns of milled samples for a) 8, b) 16, c) 24, and d) 32 h

By increasing the time to 16 h, the proportion of the SZ increases gradually at the expense of m- ZrO_2 and became the predominant phase. This is accompanied with an excessive decrease in m- ZrO_2 peaks. As a result of heat treatment, peaks are more intense and sharper than that of 8 h milling. Here, SZ will be denoted as cubic as interpreted by "highscore plus" software. Further increase in milling time to 24 h, led to the disappearance of m- ZrO_2 peaks. Single c- ZrO_2 structure with no detected m- ZrO_2 or t- ZrO_2 was obtained after 32 h of milling as indicated by the pattern. The pattern of 32 h is well consistent with JCPDS PDF No 27-0997 (space group *fm3m*, a = 0.5088 nm) which corresponds to c- ZrO_2.

Because of long milling time, contaminants (Fe, Ni, and Cr) were introduced into the powder due to wearing of milling assembly. This contamination is noted by the color of milled powder and EDX analysis. Although iron is considered as a contaminant, to some extent, its presence may be advantageous as it facilitates the mobility of Y^{3+} cations to diffuse into the m-ZrO_2 crystal lattice as reported by Sari et al. [32].

It is noted that peaks of the contaminants specially iron, were not observed in all patterns because their concentrations are below the detection limit of X-ray diffraction. Figure 7 shows EDX analysis of milled powders for 8, 16, 24, and 32 h. The level of contamination gradually increased with time. After 8 h of milling, the wt.% of Fe, Ni, and Cr were 0.7, 0.0, and 0.31 respectively. While, they were 1.33, 0.8, and 0.47 after 32 h of milling. Formation of thin layer of powder around the balls and on the interior surface of the vial results in low contamination. Also, washing of the powder with HCl removed almost the iron introduced to the powder.

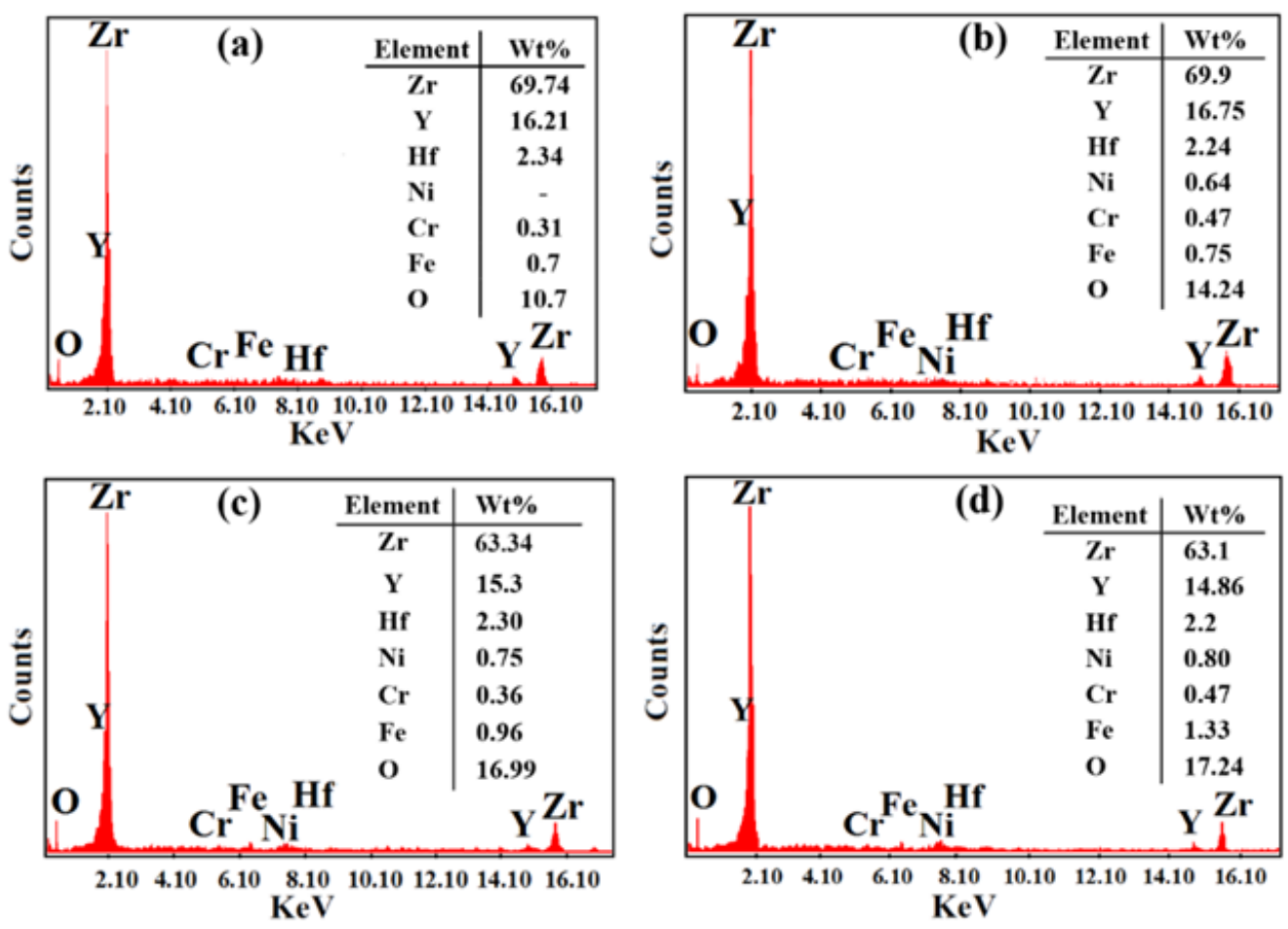

Fig. (7): EDX analysis of milled powders a) 8, b) 16, c) 24, and d) 32 h

SEM micrographs of milled powders are illustrated in figure 8. It can be seen that; all samples consist of very fine separate particles and relatively big agglomerates. Also, high resolution SEM micrograph of final powder is represented in figure 9. This figure shows that, the powder consists of submicron agglomerates which are built from very fine particles. The WH method is a convenient way for crystallite size and microstrain calculations. For the prepared ZrO_2, the calculated crystallite size and microstrain were 140 nm and 2.15×10^{-3} respectively, while they were 13.7 nm and 2.08×10^{-3} for the sample milled for 32 h. It can be clearly seen that, the values of microstrains are relatively the same because heat treatment eliminates all microstrains of milled powder. On the other hand, the crystallite size is reduced by about ten times.

Sol-gel, coprecipitation, and hydrothermal synthesis etc. are common chemical methods for the preparation of YSZ. These methods can produce YSZ with high purity and homogeneity, very fine particle size, and controllable phase structure and particle sizes. However, they are complicated, time-consuming, and too expensive in addition to the formation of large volumes of corrosive and hazardous gaseous or liquid wastes. On the other hand, MA is simple and effective and able to produce nanocrystalline materials. However, the main problem associated with MA is the introduction of contaminants into the milled powders due to wearing of milling assembly. Also, MA is considered time consuming. To overcome these two problems, YSZ milling assembly must be used to avoid contamination. Also, the milling parameters should be optimized to accelerate the process as possible to save energy.

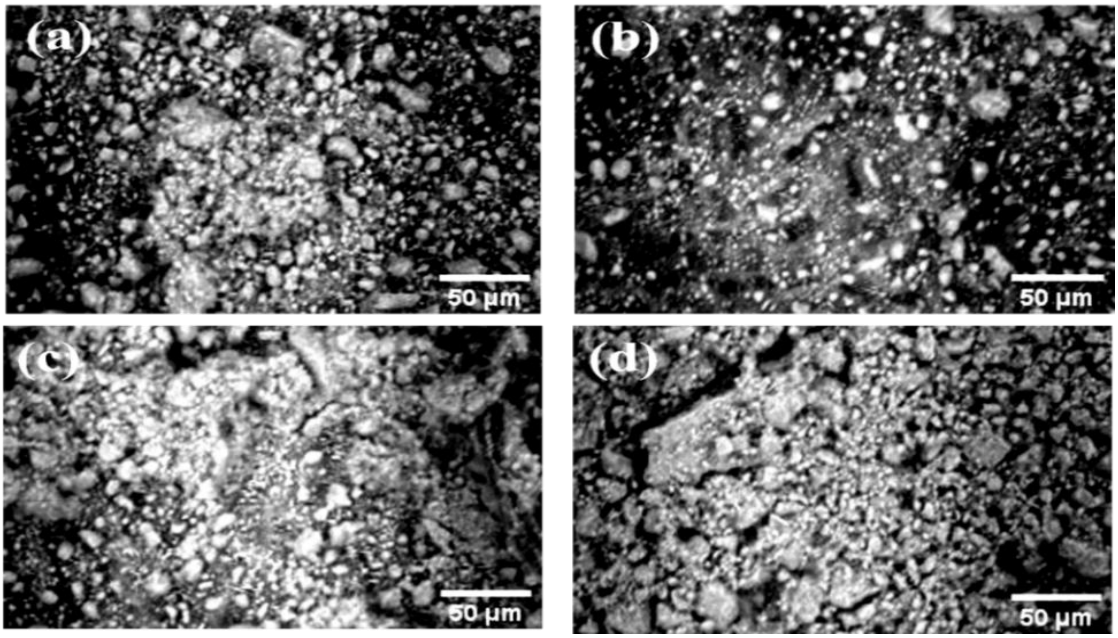

Fig. (8): SEM micrographs of milled powders for a) 8, b) 16, c) 24, and d) 32 h

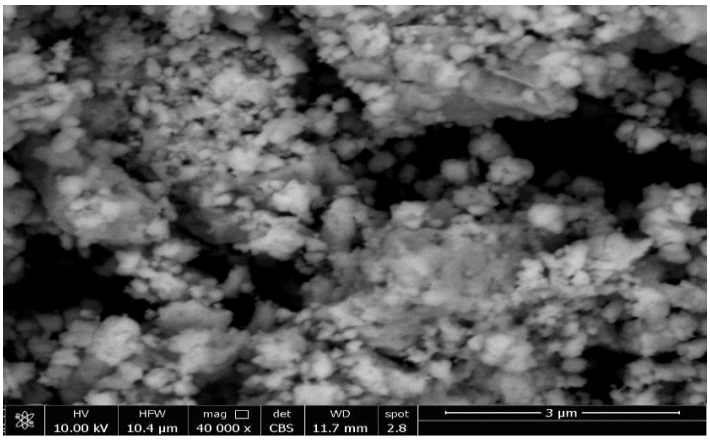

Fig. (9): High resolution SEM micrograph of milled powder for 32h

CONCLUSIONS

High purity ZrO_2 (99.62%) as the starting material for MA was successfully synthesized from Egyptian zircon. The prepared monoclinic ZrO_2 was efficiently stabilized in a cubic structure by the addition of yttria through MA with described conditions. XRD patterns show that, the degree of stabilization increases gradually with the course of milling where complete stabilization was reached at about 32 h of milling. The EDX analysis indicated that, the level of contamination increases with the increase in milling time. The produced YSZ has a good crystallinity with crystallite size in the nanometer range (13.7 nm). Also, the SEM micrograph showed that the powder is very fine and consists of submicron agglomerates.

REFERENCES

[1] Moustafa, M. I. (2007). Separation flowsheet for high-purity concentrates of some economic minerals from El Burullus-Baltim sand dunes area, North Coast, Egypt. *The Fifth International Conference on the Geology of Africa*, *1*, 107e124.

[2] Riedel, R., & Chen, I.-W. (2015). *Ceramics Science and Technology, Volume 2: Materials and Properties*. John Wiley & Sons.

[3] Askeland, D. R., Phulé, P. P., Wright, W. J., & Bhattacharya, D. K. (2003). *The science and engineering of materials*.

[4] Boch, P., & Ni, J.-C. (2010). *Ceramic Materials: Processes, Properties, and Applications* (Vol. 98). John Wiley & Sons.

[5] Zhou, G., Jin, P., Wang, Y., Pei, G., Wu, J., & Wang, Z. (2020). X-ray diffraction analysis of the yttria stabilized zirconia powder by mechanical alloying and sintering. *Ceramics International*, *46*(7), 9691–9697. https://doi.org/10.1016/j.ceramint.2019.12.236

[6] Zarkov, A., Stanulis, A., Sakaliuniene, J., Butkute, S., Abakeviciene, B., Salkus, T., Tautkus, S., Orliukas, A. F., Tamulevicius, S., & Kareiva, A. (2015). On the synthesis of yttria-stabilized zirconia: a comparative study. *Journal of Sol-Gel Science and Technology*, *76*(2), 309–319.

[7] Habashi, F. (1997). *Precious Metals. Handbook of Extractive Metallurgy, Vol III*.

[8] Reckziegel, A. (2015). Properties and applications of high-performance ceramics made of zirconia. *Aliaxis Utilities and Industry*.

[9] Farshihaghro, E. (2013). *Pyrolysis of Yttria Stabilized Zirconia and its Characterization*. UC Riverside.

[10] Shahini, S. (2017). *Design and Fabrication of Porous Yttria-Stabilized Zirconia Ceramics for Hot Gas Filtration Applications*. University of Toronto (Canada).

[11] Suryanarayana, C. (2001). Mechanical alloying and milling. *Progress in Materials Science*, *46*(1–2), 1–184. https://doi.org/10.1016/S0079-6425(99)00010-9

[12] El-Eskandarany, M. S. (2001). *Mechanical alloying: For fabrication of advanced engineering materials*. William Andrew.

[13] Zakeri, M., Razavi, M., Rahimipour, M. R., & Jamal Abbasi, B. (2014). Effect of ball to powder ratio on the ZrO_2 phase transformations during milling. *Physica B: Condensed Matter*, *444*, 49–53. https://doi.org/10.1016/j.physb.2014.03.010

[14] Sopicka-Lizer, M. (2010). *High-energy ball milling: mechanochemical processing of nanopowders*. Elsevier.

[15] Behav, S., Examiner, P., & Marcantoni, P. (2004). *(12) United States Patent*. *2*(12).

[16] Burmeister, C. F., & Kwade, A. (2013). Process engineering with planetary ball mills. *Chemical Society Reviews*, *42*(18), 7660–7667.

[17] Gajović, A., Furić, K., Štefanić, G., & Musić, S. (2005). In situ high temperature study of ZrO_2 ball-milled to nanometer sizes. *Journal of Molecular Structure*, *744*, 127–133.

[18] Jiang, J. Z., Poulsen, F. W., & Mørup, S. (1999). Structure and thermal stability of nanostructured iron-doped zirconia prepared by high-energy ball milling. *Journal of Materials Research*, *14*(4), 1343–1352.

[19] Štefanić, G., Musić, S., & Gajović, A. (2007). A comparative study of the influence of milling media on the structural and microstructural changes in monoclinic ZrO_2. *Journal of the European Ceramic Society*, *27*(2–3), 1001–1016.

[20] Musi, S., & Gajovi, A. (2007). *A comparative study of the influence of milling media on the structural and microstructural changes in monoclinic ZrO_2*. *27*, 1001–1016. https://doi.org/10.1016/j.jeurceramsoc.2006.04.136

[21] Bid, S., & Pradhan, S. K. (2002). Preparation and microstructure characterization of ball-milled ZrO_2

powder by the Rietveld method: monoclinic to cubic phase transformation without any additive. *Journal of Applied Crystallography*, *35*(5), 517–525.

[22] Bobzin, K., Zhao, L., Schlaefer, T., & Warda, T. (2011). Preparation and characterization of nanocrystalline ZrO_2-7%Y_2O_3 powders for thermal barrier coatings by high-energy ball milling. *Frontiers of Mechanical Engineering*, *6*(2), 176–181. https://doi.org/10.1007/s11465-011-0220-4

[23] Gateshki, M., Petkov, V., Williams, G., Pradhan, S. K., & Ren, Y. (2005). Atomic-scale structure of nanocrystalline ZrO_2 prepared by high-energy ball milling. *Physical Review B - Condensed Matter and Materials Physics*, *71*(22), 1–9. https://doi.org/10.1103/PhysRevB.71.224107

[24] Michel, D., Faudot, F., Gaffet, E., & Mazerolles, L. (1993). Stabilized zirconias prepared by mechanical alloying. *Journal of the American Ceramic Society*, *76*(11), 2884–2888.

[25] Dura, O. J., & de La Torre, M. A. L. (2008). X-ray diffraction line profile analysis of mechanically alloyed nanocrystalline YSZ. *Journal of Physics D: Applied Physics*, *41*(4), 45408.

[26] Zhigachev, A. O., Umrikhin, A. V., Golovin, Y. I., & Farber, B. Y. (2015). Preparation of Nanocrystalline Calcia-Stabilized Tetragonal Zirconia by High-Energy Milling of Baddeleyite. *International Journal of Applied Ceramic Technology*, *12*, E82–E89. https://doi.org/10.1111/ijac.12377

[27] Sekulić, A., Furić, K., & Stubičar, M. (1997). Raman study of phase transitions in pure and alloyed zirconia induced by ball-milling and a laser beam. *Journal of Molecular Structure*, *410*, 275–279.

[28] Sharma, A., & Ahn, B. (2018). Effect of MgO Addition on the Monoclinic to Tetragonal Transition of ZrO_2 Fabricated by High Energy Ball Milling. *Korean Journal of Metals and Materials*, *56*(10), 718–726.

[29] Chen, Y. L., Qi, M., Wu, J. S., Wang, D. H., & Yang, D. Z. (1994). Mechanical alloying process of the zirconia-8 mol % yttria ceramic powder. *Applied Physics Letters*, *65*(3), 303–305. https://doi.org/10.1063/1.113022

[30] Hao, S.-J., Wang, C., Liu, T.-L., Mao, Z.-M., Mao, Z.-Q., & Wang, J.-L. (2017). Fabrication of nanoscale yttria stabilized zirconia for solid oxide fuel cell. *International Journal of Hydrogen Energy*, *42*(50), 29949–29959.

[31] Tonejc, A. (1996). Zirconia solid solutions ZrO_2-Y_2O_3 (CoO or Fe_2O_3) obtained by mechanical alloying. *Materials Science Forum*, *225*, 497–502.

[32] Sari, A., Keddam, M., & Guittoum, A. (2015). Effect of iron impurity on structural development in ball-milled ZrO_2-3 mol% Y_2O_3. *Ceramics International*, *41*(1), 1121–1128. https://doi.org/10.1016/j.ceramint.2014.09.038